Supplementary information

Conversion and Storage of Solar Energy for Cooling

Wenbin Wang,[a] Yusuf Shi,[a] Chenlin Zhang,[a] Renyuan Li,[a] Mengchun Wu,[a] Sifei Zhuo[a], Sara Aleid,[a] Peng Wang*[a, b]

[a]Water Desalination and Reuse Center, Division of Biological and Environmental Science and Engineering, King Abdullah University of Science and Technology, Thuwal 23955-6900, Saudi Arabia. E-mail: peng.wang@kaust.edu.sa

[b]Department of Civil and Environmental Engineering, the Hong Kong Polytechnic University, Hong Kong, China

† Electronic supplementary information (ESI) available. See XXXXX

Calculation of the enthalpy of solution

The enthalpy of solution at a certain concentration is calculated as follows[1]:

$$\Delta H_{sol}^{c} = \Delta H_{sol}^{0} + L^{c} \quad \text{S1}$$

Where ΔH_{sol}^{c} (kJ mol^{-1}) is the enthalpy of solution at the solute concentration of c, ΔH_{sol}^{0} is the standard enthalpy of solution at infinite dilution, and L^{c} is the relative apparent molar enthalpy at the concentration of c.

Table S1. The solubility and enthalpy of dissolution of different salts. [1-6]

Salt	ΔH_{sat}/kJ mol^{-1} (25 °C)	Solubility (25°C) g per 100 g water
NH_4NO_3	+15.0	208.6
KNO_3	+22.2	38.3
$NaNO_3$	+10.1	91.2
NH_4Cl	+15.2	38.3
KCl	+14.3	35.7
KBr	+14.9	67.8

ΔH_{sat}: Enthalpy of saturated solution/kJ mol^{-1}

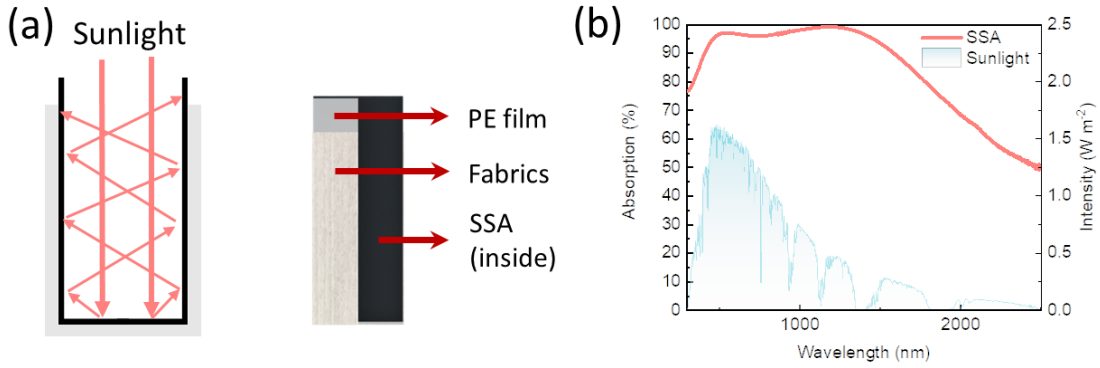

Figure S1. Design of solar solute regenerator. (a) Structure of the 3D-cup. (b) Absorption spectrum of the spectrally selective absorber (SSA) from 250 to 2,500 nm.

The spectrally selective absorber (SSA) has a high solar absorptance and low emissivity (0.1).[7] The solar absorptance (calculated from a weight fraction between incoming solar radiation energy and absorbed radiation energy) is 94% (Figure S2B). The outer wall wicking material is made by porous hydrophilic fabric and the saturated solution can be evenly distributed on its surface to form the water/air interface owing to the capillary effect. The unique property of this design is that the crystallized salt can be accumulated on the outer surface of the fabric, allowing the crystallized salt to drop off and be collected in the collector automatically.

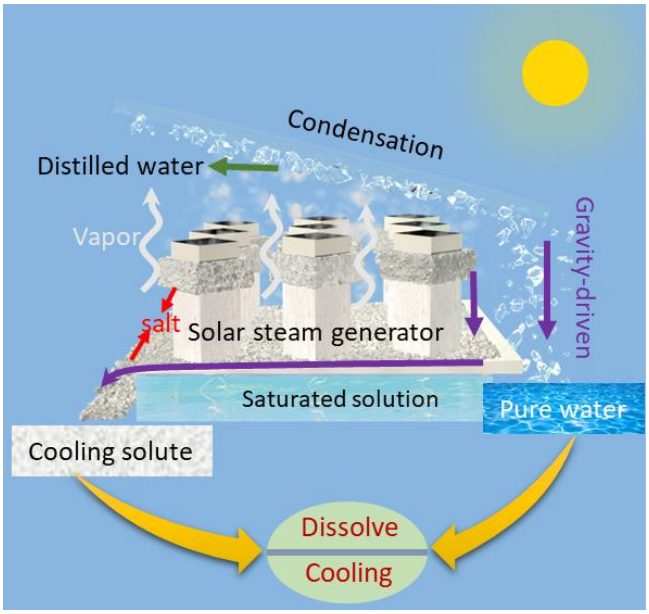

Figure S2. Recycle of water from 3D SR.

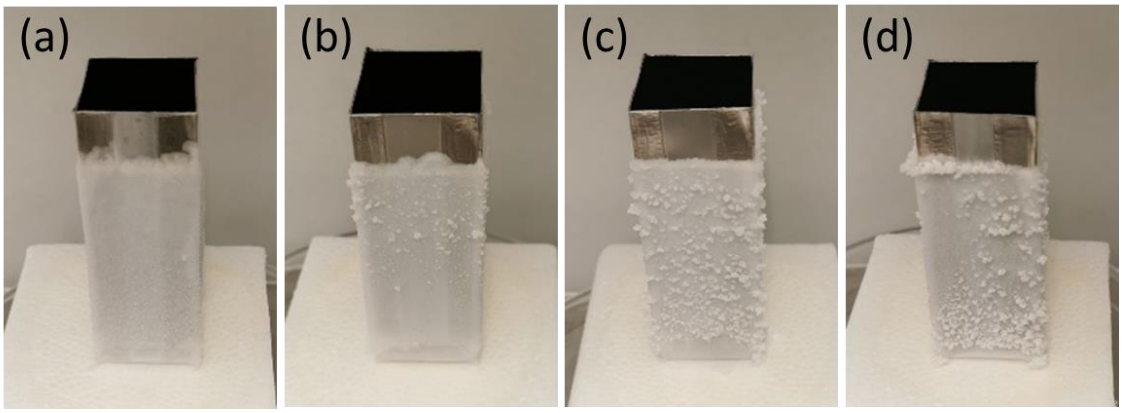

Figure S3. The crystallized NH_4NO_3 salt of the saturated NH_4NO_3 solution with the addition of sodium 4-vivylbenzenesulfonate at the concentration of (a) 0%, (b) 0.1%, (c) 0.3% and (d) 0.5%.

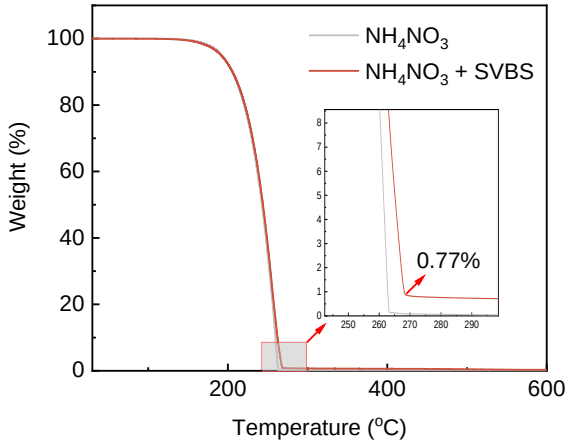

Figure S4. Thermal gravimetric analysis of the crystallized NH_4NO_3 salt obtained by the evaporation of saturated NH_4NO_3 solution with 0.5% SVBS.

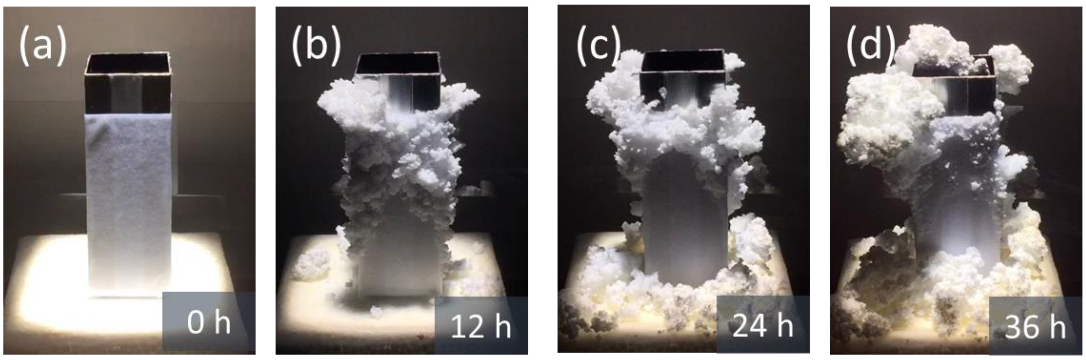

Figure S5. The crystallization process of the saturated NH_4NO_3 and 0.5% SVBS solution on the 3D -cup. (A-D) The accumulated salt on the 3D-cup.

Figure S6. The volume of pure NH_4NO_3 salt and crystallized NH_4NO_3 (with and 0.5% SVBS) with the same weight of 1 g.

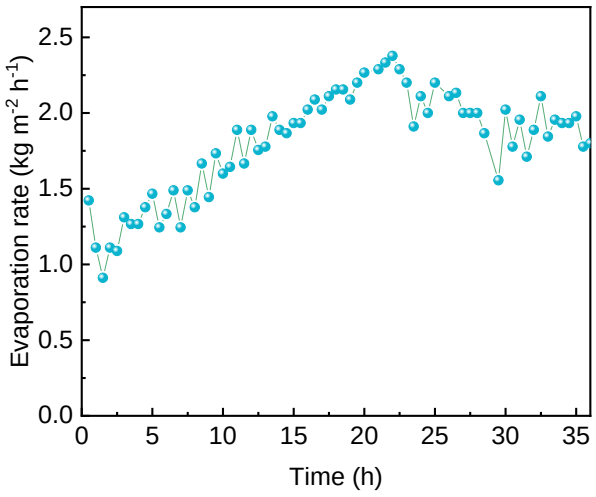

Figure S7. The evaporation rate of the saturated NH_4NO_3 solution with 0.5% SVBS on the 3D - cup.

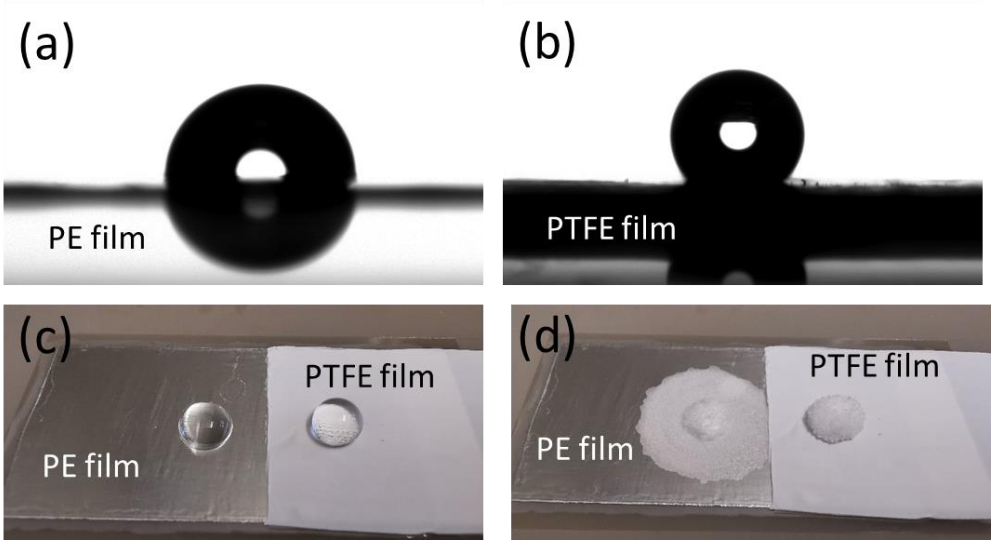

Figure S8. The crystallization of saturated NH_4NO_3 solution on polyethylene (PE) film and PTFE film. (a) the contact angle of saturated NH_4NO_3 solution on PE film and (b) PTFE film. (c-d) The crystallization process of the saturated NH_4NO_3 solution on PE film and PTFE film.

Supplementary Note S.1

Relationship between dissolution rate and heat absorption rate during dissolution

During dissolution, the heat absorption rate is governed by the dissolution rate, which can be calculated according to Noyes-Whitney equation:[8]

$$\frac{dm}{dt} = \frac{DA(C_s - C_b)}{L} \quad \text{S2}$$

Where $\frac{dm}{dt}$ is the dissolution rate (kg s^{-1}), D is the diffusion coefficient (m^2 s^{-1}), A is the surface area of the cooling solute (m^2), C_b is the concentration of the cooling solute in the bulk solution (kg m^{-3}), C_s is the particle surface concentration, which is generally believed to be equivalent to the saturated concentration, L is the diffusion layer thickness (m). As can be seen, the dissolution rate of a cooling solute can be affected by its surface area, its concentration, and temperature which affects diffusion coefficient. In comparison to pure NH_4NO_3 salt, crystallized NH_4NO_3 salt in the presence of SVBS has a higher surface area, and consequently its dissolution rate is increased. Moreover, the instant heat absorption rate or cooling power (P_{ins}) during dissolution is a function of dissolution rate and can be calculated by the following equation:

$$P_{ins} = \frac{dm}{dt} \times \frac{1000 \times \Delta H}{M} \quad \text{S3}$$

Where ΔH is the enthalpy of solution (kJ mol^{-1}). As seen, the instant cooling power can be enhanced by increasing the dissolution rate. At the beginning of dissolution, the dissolution rate is relatively high owing to the low concentration of the cooling solute in the bulk solution, leading to a rapid heat absorption. As a result, the temperature of the solution is reduced rapidly. By heat transfer, the heat of surroundings, including air, Dewar, etc., is transferred to the solution owing to their temperature disparity. When the instant cooling power is higher than the heat transfer rate, the temperature of the solution decreases. As the dissolution goes on, the concentration of the bulk solution increases, leading to a gradually decreasing dissolution rate and thus reduced instant cooling power. The cooling solution reaches a minimum temperature when the instant cooling power is equivalent to the heat transfer rate. Thereafter, the cooling power becomes lower than the heat transfer rate, and thus the solution temperature increases gradually. Meanwhile, when the solution temperature is increased, the cooling solute solubility increases, and therefore the solid

salt can continue to dissolve, slowing down the temperature rise. As a result, the system can be retained below room temperature for over 20 h in our test. These results demonstrate that the crystallized NH_4NO_3 salt in the presence of SVBS, due to its loosely accumulated structure, possesses a superior cooling performance as compared to pure NH_4NO_3 salt.

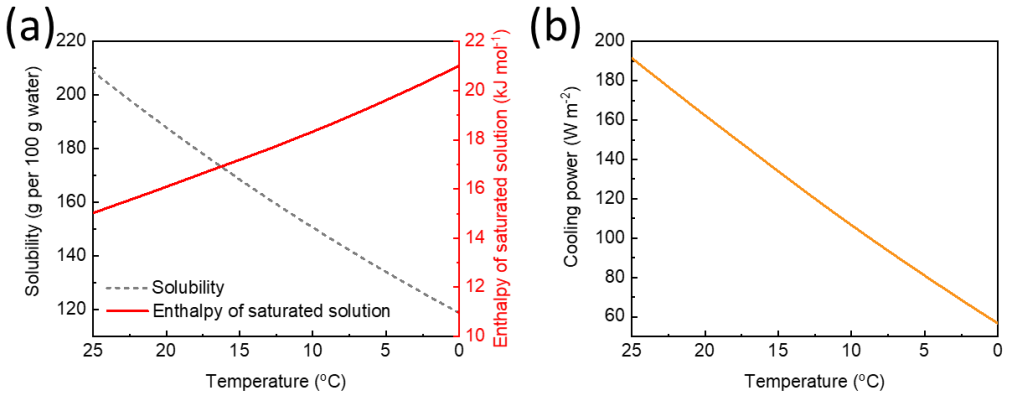

Figure S9. The evaluation of the effect of temperature on the cooling performance. (a) The effect of the temperature to the solubility, enthalpy of saturated solution of NH_4NO_3. (b) Cooling power at different temperature (Note that the ambient temperature is assumed to be 35 ^oC).

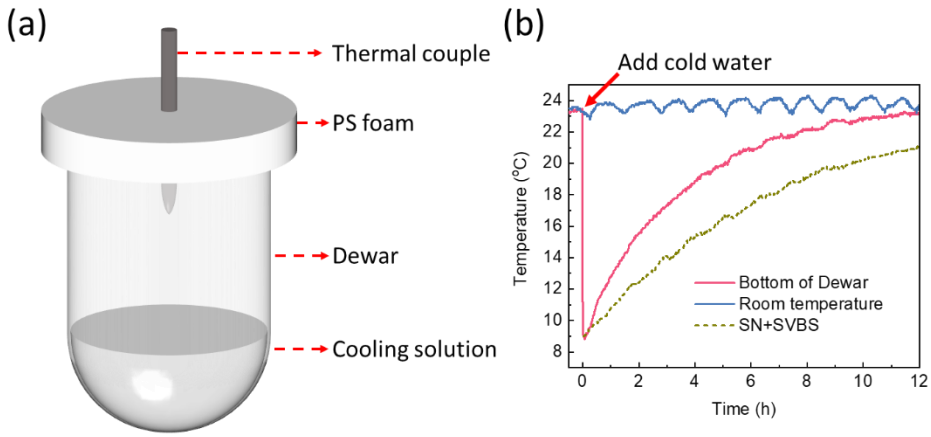

Figure S10. Cooling performance evaluation in Dewar. (a) Experimental setup for cooling performance evaluation in Dewar (note: The color of Dewar is not transparent in practical situation, it is transparent in this figure for inside observation). (b) The temperature change of the bottom of the Dewar before and after adding cold water

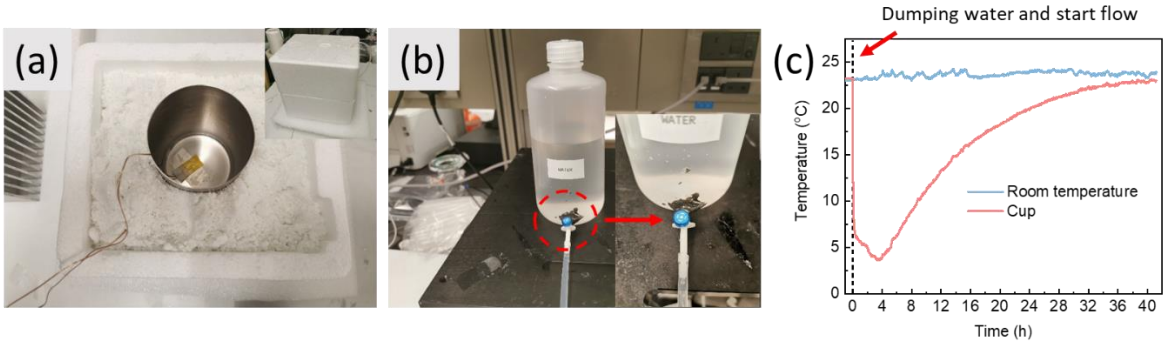

Figure S11. The cooling of the metal cup for food storage. (a) The picture of the cooling system. (b) Gravity driven flow system. (c) The temperature reduction of the cup.

Reference

1. C. Vanderzee, D. H. Waugh and N. C. Haas, Enthalpies of dilution and relative apparent molar enthalpies of aqueous ammonium nitrate. The case of a weakly hydrolysed (dissociated) salt, *J. Chem. Thermodyn*, 1980, **12**, 21-25.
2. A. W. Stelson and J. H. Seinfeld, Relative-Humidity and Temperature-Dependence of the Ammonium-Nitrate Dissociation-Constant, *Atmos. Environ*, 1982, **16**, 983-992.
3. A. Sanahuja and J. L. Gomezestevez, A New Evaluation of the Relative Apparent Molar Enthalpies of KCl in Water at 298.15 K, *Thermochim. Acta*, 1987, **117**, 105-114.
4. A. Apelblat, The Vapor-Pressures of Saturated Aqueous-Solutions of Potassium-Bromide, Ammonium-Sulfate, Copper(Ii) Sulfate, Iron(Ii) Sulfate, and Manganese(Ii) Dichloride, at Temperatures from 283 K to 308 K, *J. Chem. Thermodyn*, 1993, **25**, 1513-1520.
5. A. Apelblat and E. Korin, The vapour pressures of saturated aqueous solutions of sodium chloride, sodium bromide, sodium nitrate, sodium nitrite, potassium iodate, and rubidium chloride at temperatures from 227 K to 323 K, *J. Chem. Thermodyn*, 1998, **30**, 59-71.
6. A. Apelblat and E. Korin, Vapour pressures of saturated aqueous solutions of ammonium iodide, potassium iodide, potassium nitrate, strontium chloride, lithium sulphate, sodium thiosulphate, magnesium nitrate, and uranyl nitrate fromT=(278 to 323) K, *J. Chem. Thermodyn*, 1998, **30**, 459-471.
7. W. Wang, Y. Shi, C. Zhang, S. Hong, L. Shi, J. Chang, R. Li, Y. Jin, C. Ong and S. Zhuo, Simultaneous production of fresh water and electricity via multistage solar photovoltaic membrane distillation, *Nat. Commun*, 2019, **10**, 1-9.
8. Y. Hattori, Y. Haruna and M. Otsuka, Dissolution process analysis using model-free Noyes-Whitney integral equation, *Colloid Surface B*, 2013, **102**, 227-231.